Desalination and Water Treatment
www.deswater.com
doi: 10.5004/dwt.2021.27844

242 (2021) 117–127
December

Equilibrium, kinetic and thermodynamic studies of manganese removal from aqueous solutions by adsorption process using beet pulp shreds as a biosorbent

Jarosław Chwastowski*, Paweł Staroń

Department of Engineering and Chemical Technology, Cracow University of Technology, 24 Warszawska St., 31-155 Cracow, Poland, Tel. +48 12 628 27 11; emails: jaroslaw.chwastowski@pk.edu.pl (J. Chwastowski), pawel.staron@pk.edu.pl (P. Staroń)

Received 1 April 2021; Accepted 25 September 2021

ABSTRACT

The paper presents the adsorption abilities of organic material against manganese(II) ions. High concentrations of manganese ions cause serious damage to the environment thus novel methods for its removal are needed. The objective of the study is to use safe and natural by-product beet pulp shreds (BPS) as an adsorbent for the Mn ions adsorption from aqueous solutions. Equilibrium studies were performed to check the maximum sorption capacities of BPS against Mn ions. Kinetic calculations were used to obtain information on the effectiveness of the adsorption process. The speed, efficiency of this process were influenced by such parameters as contact time and metal ions concentration. Additionally, the influence of temperature on the course of the adsorption process was determined. Microbial studies of the BPS were performed and it was shown that there are yeast cells present in the material which in the temperature range of 20°C–30°C is characterized by their higher activity. Maximum sorption capacity for used temperatures (20°C–60°C) ranged from 4.692 to 6.800 mg/g respectively. Pseudo-second-order model, which assumes that the adsorption process is probably a chemical reaction provides the best fit.

Keywords: Kinetics; Adsorption; Manganese; Biosorbent beet pulp shreds; Thermodynamics

1. Introduction

Nowadays, many countries implicate new investments and technologies to reduce harmful compounds emitted directly to the environment like metal ions. The presence of different metals in nature is one of the main dangers and threats to various plants, as well as many animal species. Moreover, it also has a negative impact on human health. Various metals are capable of causing serious changes in the body and acute poisoning [1,2]. Different metal ions have a negative impact which may become apparent after time; this depends on the dose to which the individual has been exposed and the duration of the exposure [3]. Apart from the most toxic metals, there are transition metals like manganese which on the other hand are necessary for human health in low concentrations (daily requirement is around 2.3 mg for men and 1.8 mg for women). Unfortunately, exposures to high manganese levels are also toxic. The regulation of the minister of health on the quality of water intended for human consumption specifies the permissible amount of manganese in water at 0.05 mg Mn/dm^3. Reports of adverse health effects resulting from manganese exposure in humans are associated primarily with inhalation in occupational settings. Inhaled manganese is often transported directly to the brain before it is metabolized by the liver. The symptoms of manganese toxicity may appear slowly over months and years. Manganese toxicity can result in a permanent neurological disorder known as manganism with symptoms that include tremors, difficulty in walking, and facial muscle spasms [4].

The major anthropogenic sources of environmental manganese include municipal wastewater discharges

* Corresponding author.

sewage sludge, mining and mineral processing, emissions from alloy, steel, and iron production, combustion of fossil fuels, and emissions from the combustion of fuel additives. Manganese bearing materials such as waste batteries and spent electrodes, spent catalysts, steel scraps, sludge and slag are manganese sources that can pollute the environment. Manganese minerals are often associated with zinc sphalerite ores and nickel laterite ores, which are leached and rejected to the waste effluents in subsequent processing steps. These manganese-containing industrial waste effluents could potentially be harmful and should be controlled. The higher concentration of manganese ions also affects the environment mostly through fertilization of the water process leading to eutrophication which harms the water environment [5].

Current methods for the removal of manganese from wastewater include precipitation, ion exchange, reverse osmosis, solvent extraction, flocculation and membrane separation [6]. Oxidation and precipitation are the most common methods to remove Mn(II). Such methods are based on the Mn(II) oxidation to its insoluble manganese dioxide [7]. Conventional treatment methods for the removal of pollutants from aqueous solution, like photochemical and biological degradation, coagulation, chemical oxidation and adsorption have been investigated with varying degrees of success [8]. Among available wastewaters treatment technologies, adsorption is rapidly gaining prominence as a method of treating aqueous effluent. The most widely used adsorbent is activated carbon, but its initial cost and the need for a costly regeneration system make it less economically viable as an adsorbent.

Although the number of studies using surface-modified organic material composites has increased, the removal of Mn(II) through the adsorption process has not been investigated either with the use of waste beet pulp shreds. The paper presents adsorption models of Langmuir, Freundlich and Temkin, which can determine how metal ions are bound to the adsorbent surface. Kinetic studies are necessary to obtain information that will enable an efficient sorption process. It is also important to select appropriate concentrations of solutions and to determine the appropriate time at which the state of equilibrium is established [9]. Additionally, thermodynamic studies showed a high influence of the used temperature on sorption capacity and kinetics. Moreover, it is needed to use different organic materials such as waste beet pulp shreds obtained as a by-product after sugar production, which can be easily obtained in large quantities and at the lowest possible cost. Moreover, this material is non-toxic and biodegradable what makes it a perfect adsorbent for the removal of various metal ions from aqueous solutions. This allows for their further use in industry, for example, as biofilters useful in the process of treatment of wastewater from heavy metals.

2. Materials

2.1. Adsorbent material

Beet pulp shreds (BPS) is a matter of organic origin, 100% natural, non-toxic and biodegradable. The material came from a sugar-producing company. It is a by-product of the process of obtaining food sugar from sugar beets mostly used as fodder. The obtained material, before the sorption studies was ground in a mill and sieved (0.5 mm ϕ) to receive the unified material. The impurities contained in the BPS were removed by washing the material three times with deionized water. After the purification process shreds were dried at 30°C for 72 h.

All chemicals used in the study were of analytical grade and bought from the Sigma-Aldrich company (Germany). The solutions of manganese were prepared by dissolving the weighed amounts of manganese nitrate $Mn(NO_3)_2$ in distilled water.

2.2. Methods

2.2.1. Characterization of the adsorbent material

PBS specific surface area and total micropores volume (Brunauer–Emmet–Teller method) were measured with the use of a Macrometric ASAP 2010 analyzer. To describe the surface of the organic material SEM-EDS (Hitachi TM-3000 Scanning Electron Microscope with EDX X-ray microanalyzer) method was used. The Fourier transform infrared spectroscopy (FTIR) was used to gain information about the bonds present in the organic material. For this purpose, the Nicolet 380 Spectrometer was used.

2.2.2. Microbiological studies

The material was rinsed with autoclaved water (121°C, 2 bar) in the sterile conditions under the laminar flow chamber. In the next step 0.02 cm^3 of the filtrate was poured into the petri dish containing Sabourad agar medium and put into the heater for 24 h set at 37°C.

2.2.3. Sorption studies

Selected concentrations of manganese ions 150, 200, 250, 300 mg/dm^3 were used in the process of sorption experiments. The pH value of 6 is the natural pH of the used beet pulp shreds (Previous experiments showed that changing pH does not influence the removal process significantly – additionally, BPS has buffering properties which maintains the natural pH of the material over sorption time). The measurements were carried out in the propylene flasks with a capacity of 60 cm^3. The PBS mass used in the study was equal to 0.500 g and the volume of the model solution was 20 cm^3. The time of the experiments was equal to 1, 5, 10, 15, 30, 60 min. The observations were made based on experiments held at 20°C, 30°C, 40°C, 50°C and 60°C. At the end of the experiments, samples were filtered through the analytical filters and further analyzed with the use of atomic absorption spectrometry (AAS) to determine the concentration of manganese metal ions remaining in the filtrate. The data was obtained in triplicates and then averaged.

2.2.4. Equilibrium studies

The adsorption equilibrium has been well defined with various isotherm models relating to the amount of the solute adsorbed per unit mass of the sorbent (q_e) and

the concentration of solute in the solvent phase (C_e). To describe the sorption parameters three isotherm models were used: Langmuir, Freundlich and Temkin.

To find the best fit model for the carried out experiments the first step was to calculate the sorption capacity at the state of equilibrium q_e:

$$q_e = \frac{\left(C_0 - C_e\right)}{m} \cdot V \quad [10] \tag{1}$$

Then the sorption capacity at a given time was calculated q_t:

$$q_t = \frac{\left(C_0 - C_t\right)}{m} \cdot V \quad [11] \tag{2}$$

Using the information obtained from the above equations the calculation of the linearized form of the Langmuir isotherm was possible:

$$\frac{C_e}{q_e} = \frac{C_e}{q_{\max}} + \frac{1}{b \cdot q_{\max}} \quad [12] \tag{3}$$

Before the kinetics were established a dimensionless constant separation factor R_L was calculated which determines whether the shape of the isotherm is unfavourable ($R_L > 1$), linear ($R_L = 1$), favourable ($0 < R_L < 1$) or irreversible ($R_L = 0$) and it is calculated using the equation number 4. The separation coefficient was calculated for each concentration used in the study.

$$R_L = \frac{1}{1 + K_L \cdot C_0} \quad [13] \tag{4}$$

The percentage removal of manganese ions from solutions was calculated using Eq. (5):

$$R_e = \frac{\left(C_0 - C_e\right)}{C_e} \times 100 \quad [14] \tag{5}$$

The next isotherm model used in the study is the Freundlich isotherm model which assumes that the surface of the adsorbent material is not homogenous. From the isotherm parameter "n" one can verify if the process is of chemical or physical nature. If the value $1/n$ is below one, it indicates that the process is chemisorption.

$$\log q_e = \log K_f + \frac{1}{n} \log C_e \quad [15] \tag{6}$$

The third model used in the presented study is the Temkin isotherm model. It grants that the separate energy bonds are distributed equally until the energy of the binding is at its maximum. The equation is presented below:

$$q_e = B \ln K_t + B \ln C_e \tag{7}$$

$$B = \frac{RT}{b_t} \quad [16] \tag{8}$$

2.2.5. Sorption kinetics

Sorption kinetic study is important in wastewater treatment as it provides valuable information on the reaction pathways and the mechanism of sorption reactions. Besides, predicting the solute uptake rate is of utmost importance for designing an appropriate wastewater treatment plant since it can control the residence time of the solute at the solid-solution interface. The data modelling rate of sorption was used for the three kinetic models:

The pseudo-first rate order model

The kinetics of this equation describes the physical nature of the occurring process and is described by the linear Eq. (9):

$$\log\left(q_e - q_t\right) = \log q_e - \frac{k_1}{2.303} \cdot t \quad [17] \tag{9}$$

The pseudo-second rate order model

This model assumes that the sorption process has pseudo-chemical characteristics. The pseudo-second-order model is represented by Eq. (10):

$$\frac{t}{q_t} = \frac{t}{k_2 \cdot q_e^2} + \frac{t}{q_e} \quad [18] \tag{10}$$

Webber Morris model

The Webber-Morris model is represented by Eq. (11):

$$q_t = k_{\mathrm{id}} \cdot t^{0.5} + I \quad [19] \tag{11}$$

Thermodynamic studies

To verify the important role of the temperature in the adsorption process, studies on its influence on the sorption process were carried out. Eq. (12) was used in the calculations:

$$\Delta G = -RT \ln K_d \tag{12}$$

$$\ln K_d = -\frac{\Delta H}{RT} + \frac{\Delta S}{R} \quad [20] \tag{13}$$

To determine the spontaneity of the process, the values of thermodynamic parameters must be taken into consideration. If the process is spontaneous a decrease in $\Delta G°$ and $\Delta H°$ values with the increasing temperature. From the slope and intercept of Van't Hoff plot of $\ln K_c$ vs. $1/T$, the values of $\Delta H°$ and $\Delta S°$ can be calculated.

3. Results and discussion

3.1. Characterization of materials

Fig. 1 presents microphotographs of BPS made with scanning electron microscope with EDX analyzer.

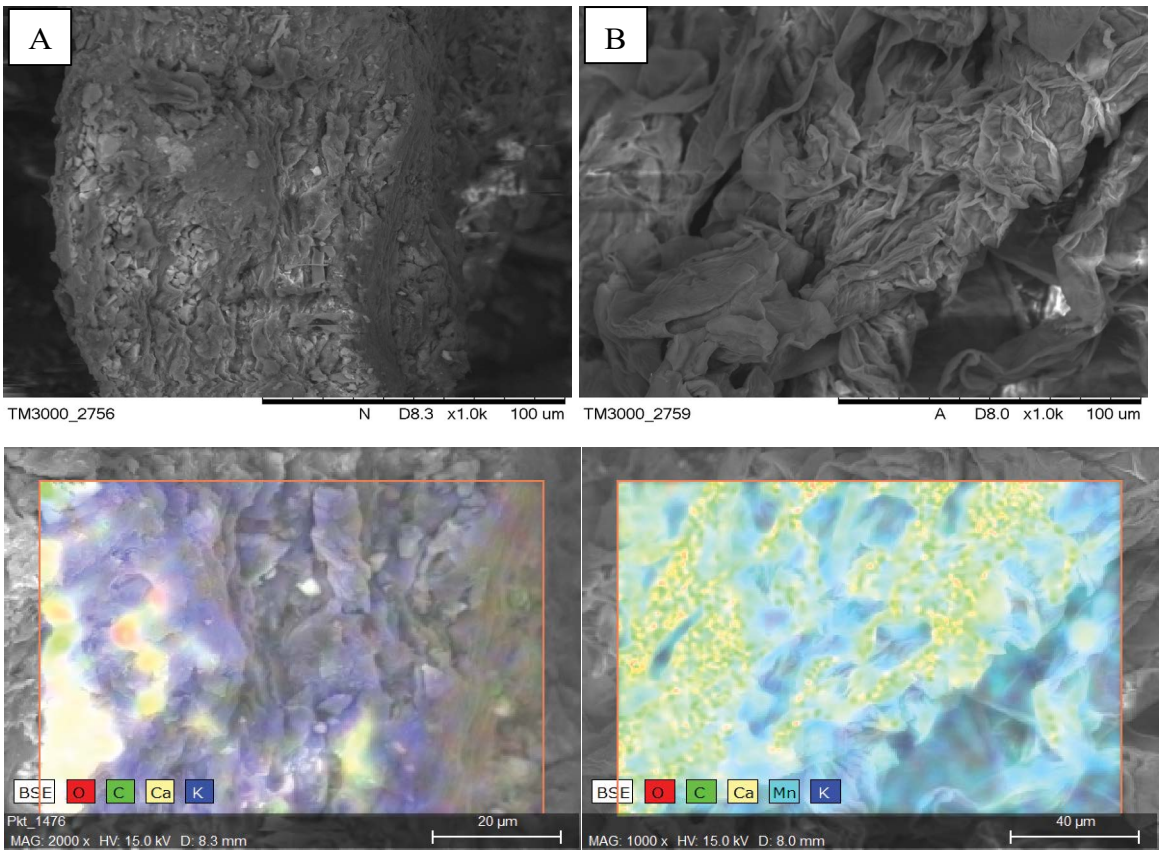

Fig. 1. SEM microphotographs (MAG x1000, x2000) and the elemental analysis of the surface of used material before (A) and after the sorption process (B).

According to SEM microphotographs, BPS has a heterogeneous, porous structure and high surface and inner porosity what is characteristic of all materials of organic origin [21]. Additionally, the EDX analysis showed that after the sorption process the manganese ions are present on the sorbent surface. The elemental compositon of the material after the sorption process is: carbon – 50.5%, oxygen – 46.87%, calcium – 1.2%, potassium 0.96%, manganese 0.82%

To check the specific surface area BET analysis was performed. The results reached 4.1244 m^2/g what is following the literature [22]. Even if the area is not as high for example as activated carbon – it can remove high concentrations of manganese ions with high affinity.

The FTIR spectra before and after the sorption of Mn(II) onto the PBS are presented in Fig. 2.

In both cases, a wide peak at 3,306 cm^{-1} suggests the presence of hydroxyl groups (OH). The characteristic sharp peak at 1,741 cm^{-1} indicates the COO^- carboxylate group. FTIR analysis of the material after the sorption process showed that the mentioned peak has a much lower intensity suggesting that carboxylate groups are probably involved in the adsorption of manganese(II) ions. The peak at the wavelength 1,004 cm^{-1} originate from NH amine groups. Additionally, there are several peaks at different wavenumbers for example 1,096 cm^{-1} (CO + OH); 1,219 cm^{-1} (C–O–C) glycosidic bond [23]; 1,370 cm^{-1} – C–H bonding and wagging and OH bonding also responsible for Mn(II) ions binding what is suggested by their lower intensity after the sorption process. This conclusion can be drawn based on the disappearance of the peak after the sorption process; 1,428 cm^{-1} –COO– symmetric stretching; 1,601 cm^{-1} – COO – anti-symmetric stretching [24]; 1,741 cm^{-1} C=O stretch in carbonyl and ester groups; region 2,900–2,938 cm^{-1} –CH stretching, CH_2 anti-symmetric stretching of methyl and methylene groups; The spectrum shows peaks which are characteristics for the cellulose structure what is following the literature [25].

3.2. Microbiological studies

On Fig. 3a Petri dish with YPD growth medium with grown cells is shown. The picture was taken 24 h after the inoculation of the probe. Colonies of yeast cells can be seen on the surface of the medium suggesting the presence of yeast cells in the PBS.

3.3. Sorption studies

To determine the sorption capacity of the used material, the equilibrium data for Mn(II) was analyzed. Fig. 4 shows the sorption capacity over time depending on the initial concentration and the degree of manganese removal.

Based on the results shown in Fig. 4 it can be concluded that the equilibrium state of sorption is achieved after about 30 min. In the initial stage of the process, the highest increase

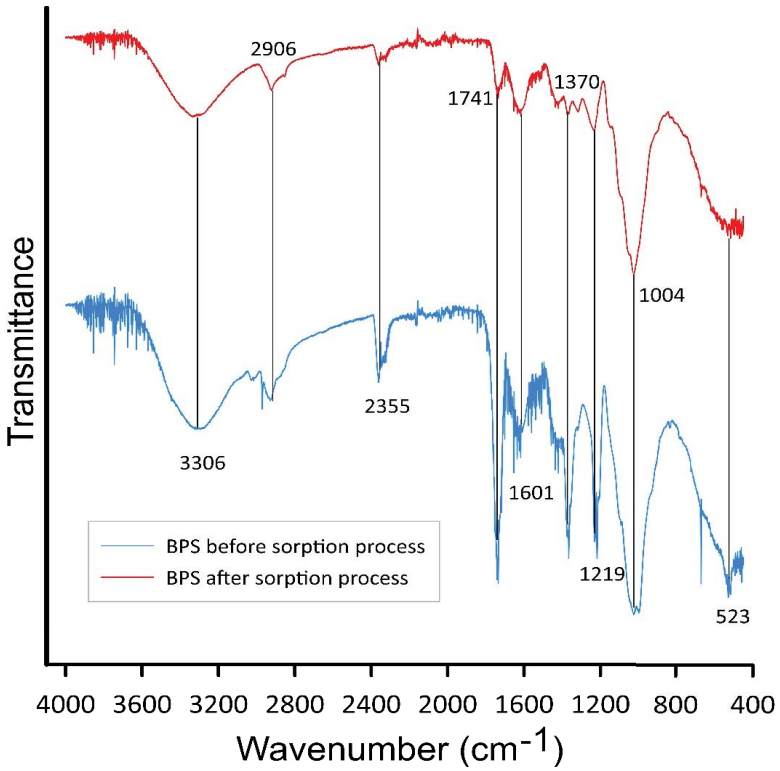

Fig. 2. The FTIR analysis of raw BPS and BPS after the Mn(II) ions sorption process.

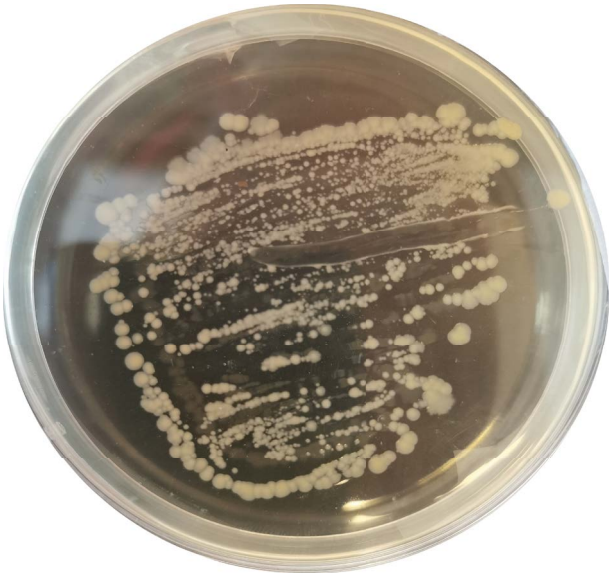

Fig. 3. Photograph of Petri dish with grown yeast cell colonies.

in the sorption capacity occur and is observed for up to 15 min. This can be related to the increase in the collisions number of manganese ions with the surface of BPS [26]

It can be seen that as the Mn(II) concentration increases the sorption capacity q_e increases as well ranging from 4.692 to 6.800 mg/g. Additionally, the percentage removal R_e ranges from 75.69 to 58.68 depending on the manganese concentration. Increasing the concentration by about 93% decreases R_e by only 22.5% suggesting that the used adsorbent has a high affinity for manganese ions. The highest removal of manganese ions can be seen at the lowest concentration used in the study. The reason is connected with the number of free active sites on the adsorbent surface which can adsorb a finite number of metal ions and a lower amount of manganese ions in the solution. Similar results have been obtained in various studies using different adsorbents [7,25–28].

3.3. Equilibrium studies

To acquire information regarding the sorption process with the use of BPS various equilibrium studies were performed. Obtained results can be modelled, projected and optimized for the process of environment bioremediation.

In Fig. 5, three used linearized form of isotherms used in the study are presented.

The parameters calculated based on isotherms are summarized in Table 1.

According to the values of the regression coefficient R^2, one can see that the Langmuir isotherm model has the best fit for the occurring sorption process at every temperature used in the experiment suggesting that a monolayer of the manganese ions on the surface of BPS is formed [29]. Langmuir constant K_L represents the affinity of adsorption sites for solute molecules and a measure of how strong solute molecule is attracted onto the adsorbent surface. Constant K_L reduces with the increasing temperature of the sorption process indicating that the decrease in temperature will

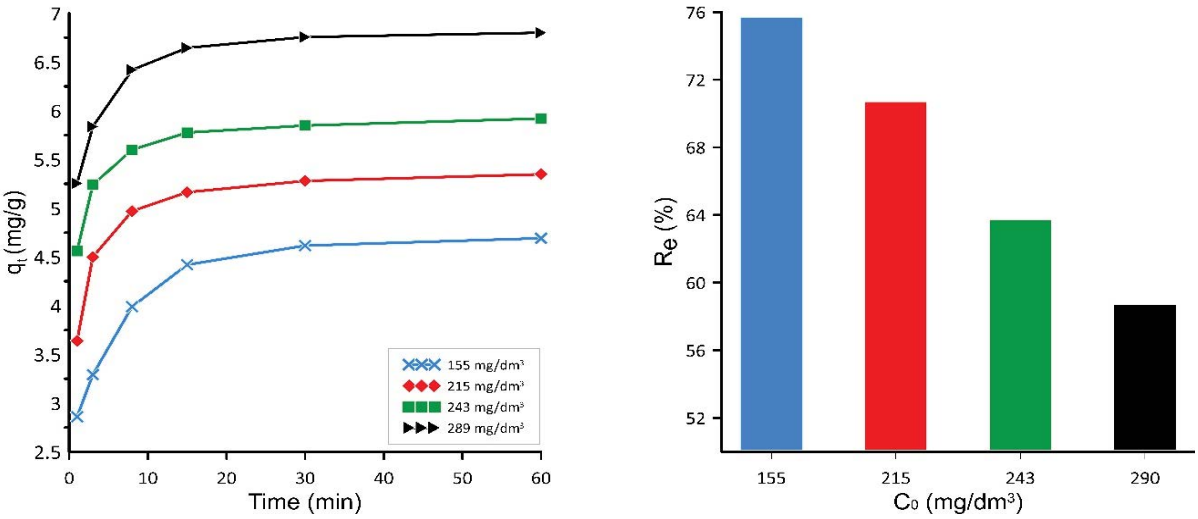

Fig. 4. Sorption capacity over specified time depending on the initial concentration (C_0) and the degree of manganese ions removal (R_e) at the temperature of 20°C.

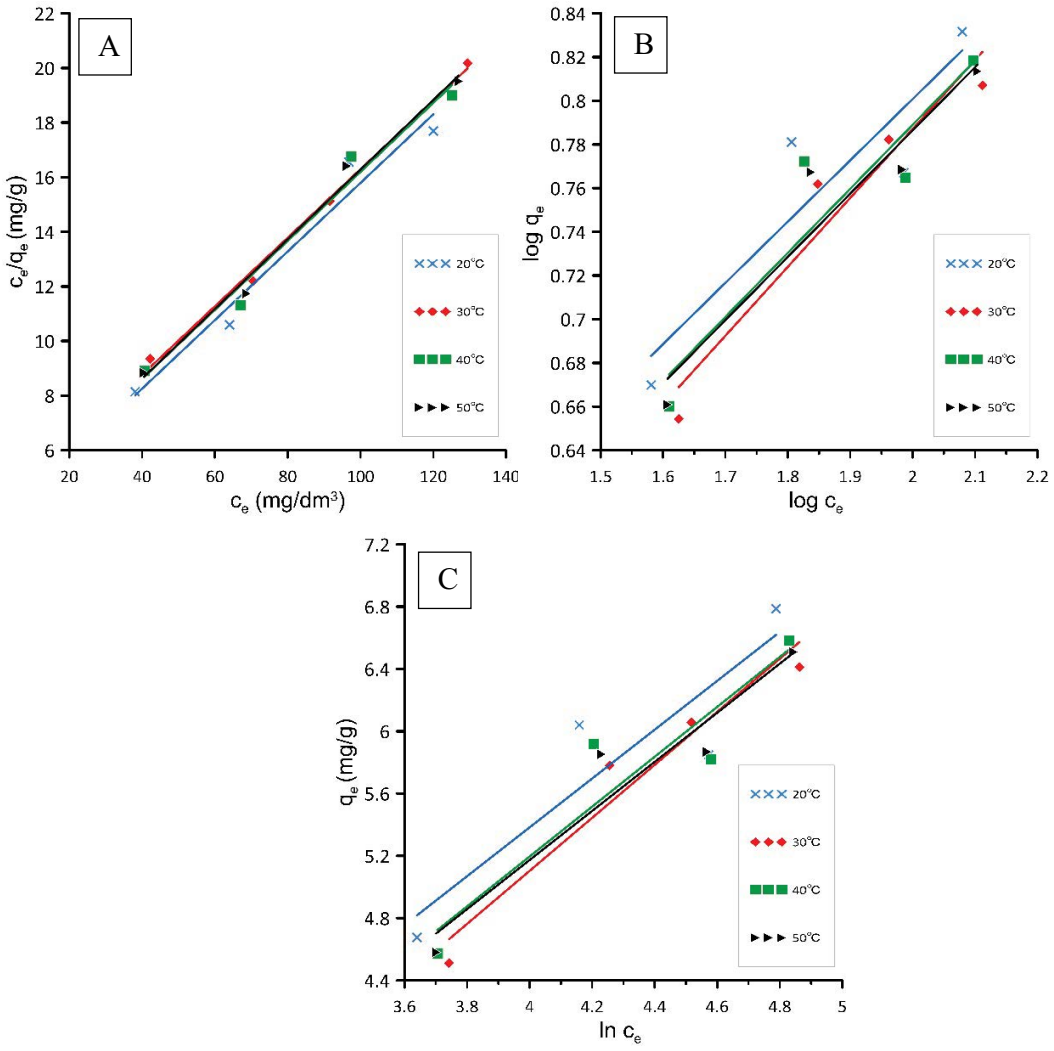

Fig. 5. Langmuir (A), Freundlich (B), and Temkin (C) isotherms of Mn(II) sorption onto PBS at different temperatures.

Table 1
Parameters and the equations of the isotherms for the sorption on BPS at varying temperatures

Isotherm models		Equations and parameters			
Langmuir		Equation	R^2	q_{max} (mg/g)	K_L (dm^3/mg)
T (°C)	20	$y = 0.1256x + 3.2311$	0.965	7.992	0.039
	30	$y = 0.1256x + 3.7382$	0.995	7.962	0.034
	40	$y = 0.1264x + 3.5575$	0.978	7.911	0.036
	50	$y = 0.1276x + 3.5214$	0.989	7.837	0.036
	60	$y = 0.1171x + 4.3390$	0.996	8.540	0.027
Freundlich		Equation	R^2	K_F (mg$^{1-(1/n)}$(dm^3)$^{1/n}$g^{-1})	$1/n$
T (°C)	20	$y = 0.2804x + 0.2399$	0.830	1.737	0.280
	30	$y = 0.3154x + 0.1563$	0.925	1.433	0.315
	40	$y = 0.2932x + 0.2027$	0.864	1.595	0.293
	50	$y = 0.2895x + 0.2074$	0.912	1.612	0.290
	60	$y = 0.3457x + 0.1011$	0.973	1.262	0.346
Temkin		Equation	R^2	K_T (dm^3/g)	B
T (°C)	20	$y = 1.5685x - 0.8912$	0.824	0.567	1.569
	30	$y = 1.7025x - 1.7064$	0.945	0.367	1.703
	40	$y = 1.6018x - 1.2118$	0.869	0.469	1.602
	50	$y = 1.5764x - 1.1327$	0.921	0.487	1.576
	60	$y = 1.8891x - 2.4857$	0.981	0.268	1.889

facilitate adsorption what is consistent with the obtained results of higher adsorption capacity at lower temperatures [30]. Additionally studying the R^2 regression coefficient R^2 (proportion of the variation in the dependent variable that is predictable from the independent variable - linear regression) for the Freundlich and Temkin models it can be seen that the obtained values are low, suggesting that those models are not suitable for characterizing the Mn(II) sorption process onto BPS.

3.4. Kinetic studies

Kinetic studies were performed to obtain information regarding the physicochemical characteristic of the occurring sorption of Mn(II) ions onto the PBS. The manganese ions sorption consists of different steps depending on various factors. To obtain the information regarding the kinetics of the Mn(II) sorption process on the beet pulp shreds, the data concerning the sorption time and initial concentration were used. Fig. 3 shows the number of metal ions sorbed in mg/g of used sorbent (BPS) against contact time using the constant mass of the sorbent. These plots show that for all solution concentrations, the number of manganese ions sorbed onto the BPS surface increases rapidly at the beginning and very slowly toward the end of the sorption. This phenomenon explains that in the first step, the metal ions are sorbed onto the surface of BPS where there are no other such molecules, and consequently, the ion-ion interactions are negligible [9].

The authors used the pseudo-first rate order model, pseudo-second rate order model and Webber–Morris model (intra-particle diffusion model) in the study (Fig. 6 and Table 2).

Observing the kinetic data in Table 2 it can be seen that the model with the best fit according to the regression coefficient R^2 is the pseudo-second kinetic order model, thus it can be assumed that the process is probably chemisorption, based on the influence of valence bonds through the sharing/exchange of electrons between manganese ions and beet pulp shreds [31] and what is following the FTIR analysis shown in Fig. 2.

3.5. Thermodynamic studies

Thermodynamic studies of the Mn(II) sorption on the BPS were carried out to verify the effect of the temperature on the sorption process. To determine the process different changes in the thermodynamic parameters must be considered (standard enthalpy ($\Delta H°$), standard entropy ($\Delta S°$), and standard free energy ($\Delta G°$)) which occur due to the transfer of unit mole of Mn(II) from solute onto the liquid-solid phase. The temperature changes will have an impact on the equilibrium constant and the sorption capacity of beet pulp shreds (Table 3) [32].

The influence of the temperature on the sorption process for different manganese ions concentrations can be examined using the data obtained from equilibrium and kinetic models.

Using the value of the K_d partition coefficient, thermodynamic parameters of the process which are; change of enthalpy ΔH, change of entropy ΔS and free energy Gibbs ΔG were calculated. The obtained results are shown in

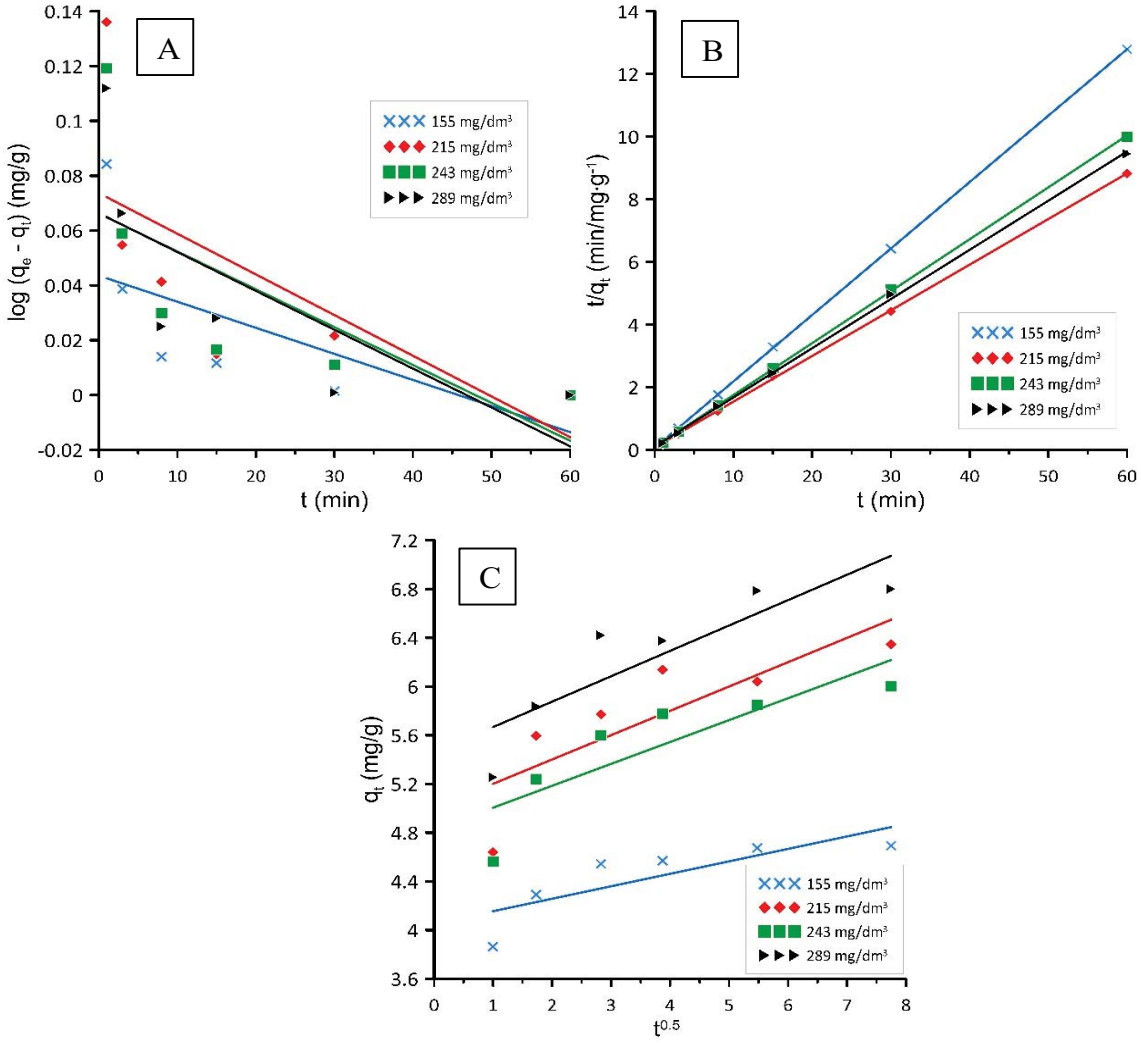

Fig. 6. Kinetics of pseudo-first-order (A), pseudo-second-order (B) and Weber–Morris (C) models for the Mn(II) sorption onto the BPS (T = 20°C).

Table 4. Studying the values of the Gibbs free energy it can be seen that at all of the tested temperatures the values are negative suggesting that the adsorption of the Mn(II) ions onto the BPS is spontaneous and feasible thermodynamically [33]. Moreover, the ΔG values are decreasing during temperature increase suggesting that the adsorption is more favourable at higher temperatures [34]. Additionally, all values of the $\Delta S°$ obtained in the study were higher than 0 suggesting that the organization of the Mn(II) ions at the phase interface during the sorption process is more random. Moreover, it can be implied that occurring phenomena are connected with the associative mechanism [35].

Examining Fig. 7 it can be seen that the adsorption of Mn(II) ions onto the PBS is a 3-way process depending on the temperature used in the test. The exothermic process was observed at the lowest temperature suggesting that microorganisms present in the material were not active (microbiological studies of the PBS were made and it was concluded that it consist of yeast cells in its structure). In the range between 30°C and 40°C, a rise can be seen in the removal capability and a change to the endothermic process which can be associated with the activation of microorganism cells. The mentioned temperature is optimal for most of the yeast cells to grow and proliferate [36]. At the temperature higher than 40°C yeast cells are degraded due to the denaturation process of proteins resulting in cell death [37]. At the temperature above 40°C process turned into the exothermic process according to the negative values of ΔH probably due to the mentioned lowered cell activity and death [33]. The negative ΔS value is connected with the decrease in the degree of freedom of adsorbed species [38].

4. Conclusion

The above study showed that beet pulp shreds have a high affinity for the Mn(II) ions and can rapidly remove them at various concentrations from aqueous solutions. The adsorption process of manganese ions on BPS was dependent on different chemical and physical parameters.

The sorption process is fast at the first minutes of the experiment and the equilibrium is reached after ~30 min. Equilibrium studies showed that the Langmuir isotherm was the best fit for all of the used temperatures (each regression coefficient R^2 was higher than 0.99). Maximum sorption capacity for used temperatures (20°C–60°C) ranged from 4.692 to 6.800 mg/g respectively. The R_L parameters for each experiment was in the range between 0 and 1 what suggest favourable conditions of the adsorption process. It can be concluded from the sorption kinetic modelling that the sorption process is best described by the pseudo-second rate order model according to the highest regression coefficient (>0.99). Thus, it can be concluded that the process is probably chemical what is under the FTIR analysis. To calculate the thermodynamic parameters thermodynamic studies were performed. The process presented in the article is both endo and exothermic process depending on the used temperature in the occurring adsorption process which is probably connected with the presence of microorganisms and their metabolic activity. Overall it can be concluded that the beet pulp shreds can be successfully used in the process of removing manganese ions from the aqueous solutions.

Table 2
Values of parameters characterizing Mn(II) sorption kinetics on BPS (T = 20°C)

Kinetics/parameters	Concentration (mg/dm^3)			
	155	215	243	290
Pseudo-first-order				
q_e (mg/g)	0.650	0.915	1.149	1.799
K_1 (min^{-1})	0.002	0.003	0.003	0.003
R^2	0.9522	0.5887	0.7604	0.9319
Pseudo-second-order				
q_e (mg/g)	4.715	6.825	7.138	12.029
K_2 (min^{-1})	0.696	0.234	0.300	0.260
R^2	1.0000	0.9992	0.9992	0.9998
Webber–Morris				
I	4.053	5.001	4.826	5.459
K_{id} (mg/g min$^{0.5}$)	0.102	0.200	0.180	0.208
R^2	0.6580	0.6792	0.7211	0.7614

Table 3
Results of the sorption capacity in the equilibrium (q_e) of the BPS for various concentrations of the Mn(II) after 60 min

T (°C)	C_0 (mg/dm^3)			
	155	215	243	290
	q_e (mg/g)			
20	4.512	5.780	6.056	6.412
30	4.676	6.040	5.848	6.786
40	4.572	5.920	5.820	6.584
50	4.580	5.852	5.868	6.508
60	4.520	5.744	5.976	6.624

Table 4
Thermodynamic parameters for the adsorption of manganese ions on BPS

Mn C_0 (mg/dm^3)	T (K)	ΔH (kJ/mol)	ΔS (J/mol K)	ΔG (kJ/mol)
	293	11.46	–56.425	–51.12
	303			–56.34
155	313	–41.11	–5.034	–56.92
	323			–58.55
	333			–61.74
	293	11.70	–59.406	–57.53
	303			–63.04
215	313	–6.22	–0.259	–63.17
	323			–63.17
	333			–69.80
	293	84.80	–51.455	–66.31
	303			–71.15
243	313	–39.90	–10.301	–72.24
	323			–74.95
	333			–78.02
	293	109.36	–61.070	–70.02
	303			–75.72
290	313	–50.10	–8.448	–76.65
	323			–79.60
	333			–82.78

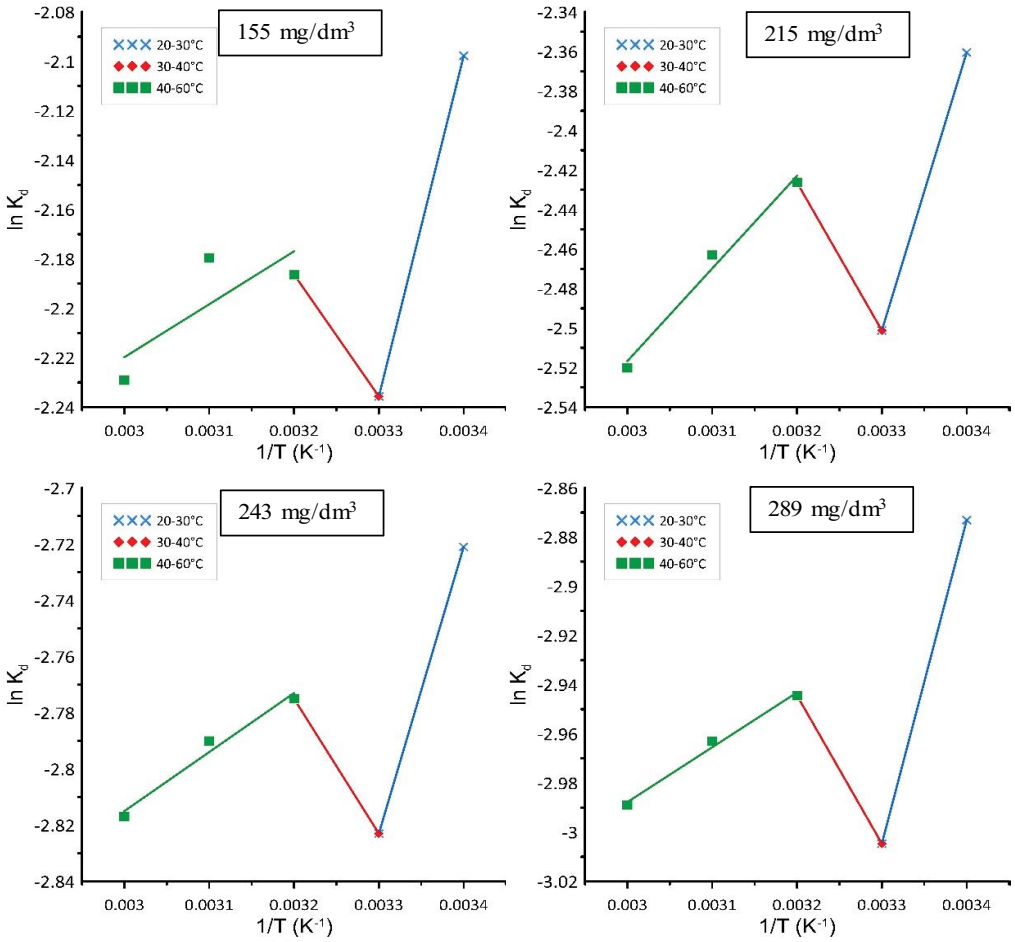

Fig. 7. Plots of lnK_d vs. 1/T for determination of thermodynamic parameters.

Symbols

BPS	—	Beet pulp shreds
C_0	—	Initial concentration of Manganese ions, mg/dm^3
C_e	—	Concentration of Manganese ions at equilibrium, mg/dm^3
q_e	—	Sorption capacity at equilibrium, mg/g
q_t	—	Sorption capacity at a given time, mg/g
m	—	Mass, g
R_e	—	The percentage removal of manganese ions at equilibrium
q_{max}	—	Maximum sorption capacity, mg/g
K_L	—	Langmuir constant, dm^3/mg
K_F	—	Freundlich constant, mg$^{1-(1/n)}$(dm^3)$^{1/n}$g^{-1}
n	—	Heterogeneity factor;
K_T	—	Equilibrium binding constant corresponding to the maximum binding energy, dm^3/g
B	—	Constant related to the heat of sorption, J/mol
b_t	—	Temkin isotherm constant;
k_1	—	Pseudo-first-order rate constant, 1/min
k_2	—	Pseudo-second-order rate constant, g/(mg·min)
k_{id}	—	Intra-particle diffusion rate constant, mg/g min$^{0.5}$
I	—	Intercept of the line in Weber–Morris model;
ΔG	—	Change of Gibbs free energy, J/mol
ΔH	—	Change of enthalpy, J/mol
ΔS	—	Change of entropy, J/mol K
K_d	—	Distribution coefficient, cm^3/g
R	—	Gas constant, J/mol K
T	—	Temperature, K

References

[1] G. Azeh Engwa, P. Udoka Ferdinand, F. Nweke Nwalo, M.N. Unachukwu, Mechanism and Health Effects of Heavy Metal Toxicity in Humans, O. Karcioglu, B. Arslan, Eds., Poisoning in the Modern World – New Tricks for an Old Dog?, IntechOpen, 2019, doi: 10.5772/intechopen.82511. Available at: https://doi.org/10.5772/intechopen.82511.

[2] H. Ali, E. Khan, I. Ilahi, Environmental chemistry and ecotoxicology of hazardous heavy metals: environmental persistence, toxicity, and bioaccumulation, J. Chem., 2019 (2019) 1–14, doi: 10.1155/2019/6730305.

[3] M. Jaishankar, T. Tseten, N. Anbalagan, B.B. Mathew, K.N. Beeregowda, Toxicity, mechanism and health effects of some heavy metals, Interdiscip. Toxicol., 7 (2014) 60–72.

[4] K. Prabhakaran, A.B. Bowman, M. Xilouri, D.S. Harischandra, S. Ghaisas, G. Zenitsky, H. Jin, A. Kanthasamy, V. Anantharam, A.G. Kanthasamy, Manganese-induced neurotoxicity: new insights into the triad of protein misfolding, mitochondrial impairment, and neuroinflammation, Front. Neurosci., 13 (2019) 654, doi: 10.3389/fnins.2019.00654.
[5] C.D. Giles, P.D.F. Isles, T. Manley, Y. Xu, G.K. Druschel, A.W. Schroth, The mobility of phosphorus, iron, and manganese through the sediment–water continuum of a shallow eutrophic freshwater lake under stratified and mixed water-column conditions, Biogeochemistry, 127 (2016) 15–34.
[6] O.A. Oyewo, O. Agboola, M.S. Onyango, P. Popoola, M.F. Bobape, Chapter 6 – Current Methods for the Remediation of Acid Mine Drainage Including Continuous Removal of Metals From Wastewater and Mine Dump, M.N.V. Prasad, P.J. de Campos Favas, S.K. Maiti, Eds., Bio-Geotechnologies for Mine Site Rehabilitation, Elsevier, 2018, pp. 103–114.
[7] S. Kouzour, N. El Azher, B. Gourich, F. Gros, C. Vial, Y. Stiriba, Removal of manganese(II) from drinking water by aeration process using an airlift reactor, J. Water Process Eng., 16 (2017) 233–239.
[8] I.A. Saleh, N. Zouari, M.A. Al-Ghouti, Removal of pesticides from water and wastewater: chemical, physical and biological treatment approaches, Environ. Technol. Innovation, 19 (2020) 101026, doi: 10.1016/j.eti.2020.101026.
[9] P. Staroń, J. Chwastowski, M. Banach, Sorption behavior of methylene blue from aqueous solution by raphia fibers, Int. J. Environ. Sci. Technol., 16 (2019) 8449–8460.
[10] S.-Y. Yoon, C.-G. Lee, J.-A. Park, J.-H. Kim, S.-B. Kim, S.-H. Lee, J.-W. Choi, Kinetic, equilibrium and thermodynamic studies for phosphate adsorption to magnetic iron oxide nanoparticles, Chem. Eng. J., 236 (2014) 341–347.
[11] M. Auta, B.H. Hameed, Chitosan–clay composite as highly effective and low-cost adsorbent for batch and fixed-bed adsorption of methylene blue, Chem. Eng. J., 237 (2014) 352–361.
[12] S. Ghorbani-Khosrowshahi, M.A. Behnajady, Chromium(VI) adsorption from aqueous solution by prepared biochar from Onopordom Heteracanthom, Int. J. Environ. Sci. Technol., 13 (2016) 1803–1814.
[13] M. Shaban, M.R. Abukhadra, A.A.P. Khan, B.M. Jibali, Removal of Congo red, methylene blue and Cr(VI) ions from water using natural serpentine, J. Taiwan Inst. Chem. Eng., 82 (2018) 102–116.
[14] S. Kaur, S. Rani, R.K. Mahajan, M. Asif, V.K. Gupta, Synthesis and adsorption properties of mesoporous material for the removal of dye safranin: kinetics, equilibrium, and thermodynamics, J. Ind. Eng. Chem., 22 (2015) 19–27.
[15] V.S. Munagapati, D.-S. Kim, Equilibrium isotherms, kinetics, and thermodynamics studies for congo red adsorption using calcium alginate beads impregnated with nano-goethite, Ecotoxicol. Environ. Saf., 141 (2017) 226–234.
[16] V.O. Njoku, K.Y. Foo, M. Asif, B.H. Hameed, Preparation of activated carbons from rambutan (*Nephelium lappaceum*) peel by microwave-induced KOH activation for acid yellow 17 dye adsorption, Chem. Eng. J., 250 (2014) 198–204.
[17] J.-P. Simonin, On the comparison of pseudo-first-order and pseudo-second-order rate laws in the modeling of adsorption kinetics, Chem. Eng. J., 300 (2016) 254–263.
[18] P. Lukes, E. Dolezalova, I. Sisrova, M. Clupek, Aqueous-phase chemistry and bactericidal effects from an air discharge plasma in contact with water: evidence for the formation of peroxynitrite through a pseudo-second-order post-discharge reaction of H_2O_2 and HNO_2, Plasma Sources Sci. Technol., 23 (2014) 015019, doi: 10.1088/0963-0252/23/1/015019.
[19] Y. Yang, X. Lin, B. Wei, Y. Zhao, J. Wang, Evaluation of adsorption potential of bamboo biochar for metal-complex dye: equilibrium, kinetics and artificial neural network modeling, Int. J. Environ. Sci. Technol., 11 (2014) 1093–1100.
[20] M. Shahverdi, E. Kouhgardi, B. Ramavandi, Characterization, kinetic, and isotherm data for Cr(VI) removal from aqueous solution by *Populus alba* biochar modified by a cationic surfactant, Data Brief, 9 (2016) 163–168.
[21] Y.N. Mata, M.L. Blázquez, A. Ballester, F. González, J.A. Muñoz, Sugar-beet pulp pectin gels as biosorbent for heavy metals: Preparation and determination of biosorption and desorption characteristics, Chem. Eng. J., 150 (2009) 289–301.
[22] V.M. Dronnet, C.M.G.C. Renard, M.A.V. Axelos, J.F. Thibault, Binding of divalent metal cations by sugar-beet pulp, Carbohydr. Polym., 34 (1997) 73–82.
[23] K.Y. Andrew Lin, Y.T. Hsieh, Copper-based metal organic framework (MOF), HKUST-1, as an efficient adsorbent to remove p-nitrophenol from water, J. Taiwan Inst. Chem. Eng., 50 (2015) 223–228.
[24] A.S. Yusuff, L.T. Popoola, E.O. Babatunde, Adsorption of cadmium ion from aqueous solutions by copper-based metal organic framework: equilibrium modeling and kinetic studies, Appl. Water Sci., 9 (2019) 3, doi: 10.1007/s13201-019-0991-z.
[25] V. Hospodarova, E. Singovszka, N. Stevulova, Characterization of cellulosic fibers by FTIR spectroscopy for their further implementation to building materials, Am. J. Anal. Chem., 9 (2018) 303–310.
[26] J.L. Chen, L. Gao, Q. Jiang, Q. Hou, Y. Hong, W. Jian Shen, Y. Wang, J.H. Zhu, Fabricating efficient porous sorbents to capture organophosphorus pesticide in solution, Microporous Mesoporous Mater., 294 (2020) 109911, doi: 10.1016/j.micromeso.2019.109911.
[27] V.A. Pacini, A.M. Ingallinella, G. Sanguinetti, Removal of iron and manganese using biological roughing up flow filtration technology, Water Res., 39 (2005) 4463–4475.
[28] A. Bin Jusoh, W.H. Cheng, W.M. Low, A. Nora'aini, M.J. Megat Mohd Noor, Study on the removal of iron and manganese in groundwater by granular activated carbon, Desalination, 182 (2005) 347–353.
[29] J. Chwastowski, D. Bradło, W. Żukowski, Adsorption of cadmium, manganese and lead ions from aqueous solutions using spent coffee grounds and biochar produced by its pyrolysis in the fluidized bed reactor, Materials (Basel), 13 (2020) 2782, doi: 10.3390/ma13122782.
[30] Q. Hu, Y. Liu, C. Feng, Z. Zhang, Z. Lei, K. Shimizu, Predicting equilibrium time by adsorption kinetic equations and modifying Langmuir isotherm by fractal-like approach, J. Mol. Liq., 268 (2018) 728–733.
[31] T. Gupta, A.K. Agarwal, R.A. Agarwal, N.K. Labhsetwar, Environmental Contaminants: Measurement, Modelling and Control, Springer Nature Singapore Pte Ltd., 2014.
[32] Z.A. AL-Othman, R. Ali, M. Naushad, Hexavalent chromium removal from aqueous medium by activated carbon prepared from peanut shell: adsorption kinetics, equilibrium and thermodynamic studies, Chem. Eng. J., 184 (2012) 238–247.
[33] Z. Duan, M. Song, T. Li, S. Liu, X. Xu, R. Qin, C. He, Y. Wang, L. Xu, M. Zhang, Characterization and adsorption properties of cross-linked yeast/β-cyclodextrin polymers for Pb(II) and Cd(II) adsorption, 8 (2018) 31542–31554.
[34] N. Rahman, U. Haseen, Equilibrium modeling, kinetic, and thermodynamic studies on adsorption of Pb(II) by a hybrid inorganic–organic material: polyacrylamide zirconium(IV) iodate, Ind. Eng. Chem. Res., 53 (2014) 8198–8207.
[35] A. Davarpanah, B. Mirshekari, Experimental investigation and mathematical modeling of gas diffusivity by carbon dioxide and methane kinetic adsorption, Ind. Eng. Chem. Res., 58 (2019) 12392–12400.
[36] R. Gao, Z. Li, X. Zhou, S. Cheng, L. Zheng, Oleaginous yeast *Yarrowia lipolytica* culture with synthetic and food waste-derived volatile fatty acids for lipid production, Biotechnol. Biofuels, 10 (2017) 247, doi: 10.1186/s13068-017-0942-6.
[37] P. Staroń, J. Chwastowski, M. Banach, Sorption and desorption studies on silver ions from aqueous solution by coconut fiber, J. Cleaner Prod., 149 (2017) 290–301.
[38] S. Lombardo, A. Gençeŗ, C. Schütz, J. Van Rie, S. Eyley, W. Thielemans, Thermodynamic study of ion-driven aggregation of cellulose nanocrystals, Biomacromolecules, 20 (2019) 3181–3190.